6. On the Technique and the Analysis of Transient Maneuver Tests

Masami HAMAMOTO*, Kazuhiko HASEGAWA*, and Takashi IIDA**

(From J.S.N.A. Japan, Vol. 161, June 1987)

Summary

A new transient maneuver test designed to measure the hydrodynamic derivatives of a maneuvering ship has been developed. These tests were carried out using the planar motion mechanism. The forces acting on a model are decomposed into the added mass and the damping forces using linear systems analysis. Experiment results are analysed by a new method using a transfer function approximation and compared with the analysis by the Kramers–Kronig relations.

1. Introduction

A planar motion mechasism (P.M.M.) introduced by Gertler (1959)[1] and Goodman (1960)[2] is a device which forces an oscillatory motion in a horizontal plane to a model during being towed at constant speed. Van Leeuwen (1964)[3] and Motora and Fujino (1965)[4] carried out the forced pure sway and pure yaw tests to evaluate the hydrodynamic forces and moments acting on an oscillatory model. The experiment results indicate that the hydrodynamic forces and moments are influenced by the frequency of motion.

The theoretical approach for this frequency dependence have been conducted by Cummins (1962)[5] in free surface effects and by Brard (1964)[6] in the development of a vortex theory for a submerged maneuvering body. Following their considerations, the frequency dependence is found to come from the fact that the hydrodynamic forces and moments acting on a ship are influenced by her previous motion. The influence appeared in the time history and that in the range of frequency is equivalent, if the motion is composed of various amplitude and frequency sine waves. The same is true for non–periodical motion. This is shown by taking Fourier transform of the hydrodynamic force caused by a transient motion where the motion will disappear after reasonable time. A transient motion contains energy which, in general, is distributed over a range of frequency. Thus a single motion can provide information about the hydrodynamic forces at any frequency of interest. Frank (1976)[7] has proposed a new technique that is a more efficient use of the planar motion mechanism than the usual frequency–by–frequency testing and reported the results of some experiments employing the proposed technique.

This paper is concerned with the technique and the analysis of such experiments. The authors will investigate an important relationship between the hydrodynamic derivatives, which is called the Kramers–Kronig relations. For this purpose, they have designed a P.M.M. for transient maneuver tests and then carried out captive model tests to investigate the property of hydrodynamic forces acting on a ship in transient state. The experiment results are discussed based on linear systems analysis. An approximation of transfer function is introduced for the analysis of complex frequency response function obtained from the experiments.

2. Equations of Motion

For a maneuvering ship with the body axes located at the center of gravity, the equations of

* Department of Naval Architecture, Osaka University

** Graduate School, Department of Naval Architecture, Osaka University

motion may be described as:

$$m(\dot{u}-vr)=-\iint_s pn_x dS+X$$

$$m(\dot{v}+ur)=-\iint_s pn_y dS+Y \quad (1)$$

$$I_z\dot{r}=-\iint_s p(xn_y-yn_x)dS+N$$

where m and I_z denote the mass and moment of inertia about the yaw axis of the ship; u and v the linear forward and swaying velocities; r the angular yawing velocity; p the hydrodynamic pressure acting on the submerged surface S; n_x and n_y the components of unit normal vectors pointing out of the ship's surface; and X, Y and N the external forces and yawing moment.

The main problem is to evaluate the pressure integrals on the right hand side of Eq. (1). The hydrodynamic pressure acting on a maneuvering ship is partly due to circulation around the ship. This generates a vortex wake because the circulation along a closed fluid circuit is null. It would be interesting to investigate the transport mechanism of vorticity from the boundary layer into the wake. Unfortunately, a full theoretical derivation is very difficult at the present time. Alternatively, we have chosen an experimental approach based on linear systems analysis.

By assuming that perturbed velocities result from a uniform forward velocity U, and since the surge equation is not coupled to the sway and yaw equations, one obtains linearized equations of motion:

$$m(\dot{v}+Ur)+\iint_s p(\mathrm{sway})n_y dS$$

$$+\iint_s p(\mathrm{yaw})n_y dS=Y$$

$$I_z\dot{r}+\iint_s p(\mathrm{sway})(xn_y-yn_x)dS$$

$$+\iint_s p(\mathrm{yaw})(xn_y-yn_x)dS=N \quad (2)$$

where p(sway) and p(yaw) denote the linearized pressure acting on a ship with pure sway and yaw motions. Y and N are the external force and moment.

3. Linear Systems Analysis to Evaluate Pressure Integrals

The pressure integrals in Eq. (2) need to be determined. However, we can treat them as a "black box" in linear systems analysis, since we are interested in the system's input–output behavior but not in the hydrodynamical background.

System response to a unit impulse $\delta(t)$ is known as the impulse response. In this case, the input signal $x(t)$ can be written as a convolution integral:

$$x(t)=\int_{-\infty}^{\infty}x(\tau)\delta(t-\tau)d\tau \quad (3)$$

for a linear time–invariant system whose impulse response is $g(t)$. The output signal $y(t)$ corresponding to the input signal $x(t)$ is:

$$y(t)=G[x(t)]$$

$$=\int_{-\infty}^{\infty}x(\tau)G[\delta(t-\tau)]d\tau$$

$$=\int_{-\infty}^{\infty}x(\tau)g(t-\tau)d\tau \quad (4)$$

where $G[\ ]$ denotes the system transfer operator.

Taking the Fourier transform of Eq. (4), one obtains:

$$\hat{y}(\omega)=\hat{x}(\omega)\hat{g}(\omega) \quad (5)$$

where $\hat{g}(\omega)$ is a frequency response function defined as

$$\hat{y}(\omega)=\int_{-\infty}^{\infty}y(t)e^{-i\omega t}dt \quad (6)$$

$$\hat{x}(\omega)\hat{g}(\omega)=\int_{-\infty}^{\infty}\left[\int_{-\infty}^{\infty}x(\tau)g(t-\tau)\,d\tau\right]e^{-i\omega t}dt$$

$$= \int_{-\infty}^{\infty} x(\tau) e^{-i\omega\tau} d\tau$$

$$\times \int_{-\infty}^{\infty} g(t-\tau) e^{-i\omega(t-\tau)} dt \tag{7}$$

Therefore, if one measures the time histories of the input and the output signals, he can evaluate the frequency response function as:

$$\hat{g}(\omega) = \frac{\hat{y}(\omega)}{\hat{x}(\omega)} = \frac{y_c x_c + y_s x_s}{x_c^2 + x_s^2}$$

$$+ i \frac{y_c x_s - y_s x_c}{x_c^2 + x_s^2} \tag{8}$$

where

$$\hat{y}(\omega) = y_c - i y_s ,$$

$$\hat{x}(\omega) = x_c - i x_s$$

$$y_c(\omega) = \int_{-\infty}^{\infty} y(t) \cos \omega t \; dt ,$$

$$y_s(\omega) = \int_{-\infty}^{\infty} y(t) \sin \omega t \; dt$$

$$x_c(\omega) = \int_{-\infty}^{\infty} x(t) \cos \omega t \; dt ,$$

$$x_s(\omega) = \int_{-\infty}^{\infty} x(t) \sin \omega t \, dt \tag{9}$$

For causal systems, the Kramers–Kronig relations between the real part $\mathrm{Re}[\hat{g}(\omega)]$ and imaginary part $\mathrm{Im}[\hat{g}(\omega)]$ of the frequency response function $\hat{g}(\omega) = \mathrm{Re}[\hat{g}(\omega)] + i\,\mathrm{Im}[\hat{g}(\omega)]$ is:

$$Re[\hat{g}(\omega)] = \frac{1}{\pi} \int_{-\infty}^{\infty} \frac{Im[\hat{g}(k)]}{\omega - k} dk$$

$$Im[\hat{g}(\omega)] = -\frac{1}{\pi} \int_{-\infty}^{\infty} \frac{Re[\hat{g}(k)]}{\omega - k} dk \tag{10}$$

From Eq. (8) the input–output relation in the frequency domain can be given as:

$$\frac{Im[\hat{g}(\omega)]}{\omega} \hat{\hat{x}}(\omega)$$

$$+ Re[\hat{g}(\omega)] \hat{x}(\omega) = \hat{y}(\omega) \tag{11}$$

where $\hat{\hat{x}}(\omega) = i\omega\hat{x}(\omega)$ is the Fourier transform of the differential of $x(t)$ with respect to time t.

Likewise, $Re[\hat{g}(\omega)]$ and $Im[\hat{g}(\omega)]$ can be represented as the real part and imaginary part of transfer function $\hat{g}(s)$ by setting $s = i\omega$. If the transfer function is written as[8]:

$$\hat{g}(s) = \frac{k(s+c)(s^2 + 2as + b^2)}{s^2 + 2\alpha s + \beta^2} \tag{12}$$

$Re[\hat{g}(\omega)]$ and $Im[\hat{g}(\omega)]$ can be represented as

$$Re[\hat{g}(\omega)] =$$

$$k \left\{ \frac{c[(b^2 - \omega^2)(\beta^2 - \omega^2) + 4\omega^2 a \alpha]}{(\beta^2 - \omega^2)^2 + 4\omega^2 \alpha^2} \right.$$

$$\left. - \frac{2\omega^2 [a(\beta^2 - \omega^2) - \alpha(b^2 - \omega^2)]}{(\beta^2 - \omega^2)^2 + 4\omega^2 \alpha^2} \right\} \tag{13}$$

and

$$\frac{Im[\hat{g}(\omega)]}{\omega}$$

$$= k \left\{ \frac{(b^2 - \omega^2)(\beta^2 - \omega^2) + 4\omega^2 a \alpha}{(\beta^2 - \omega^2)^2 + 4\omega^2 \alpha^2} \right.$$

$$\left. - \frac{2c[a(\beta^2 - \omega^2) - \alpha(b^2 - \omega^2)]}{(\beta^2 - \omega^2)^2 + 4\omega^2 \alpha^2} \right\} \tag{14}$$

The impulse response function is derived from Eq. (12) as:

$$g(t) = k\dot{\delta}(t) + k(c + 2a - 2\alpha)\delta(t)$$

$$+ k[(b^2 - \beta^2) + 2(c - 2\alpha)(a - \alpha)]$$

$$\times e^{-\alpha t} \cos(\beta^2 - \alpha^2)^{1/2} t + k$$

$$\times \frac{(c-\alpha)(b^2 - \beta^2) - 2(c\alpha + \beta^2 - 2\alpha^2)(a - \alpha)}{(\beta^2 - \alpha^2)^{1/2}}$$

$$\times e^{-\alpha t}\sin(\beta^2-\alpha^2)^{1/2}t \tag{15}$$

Furthermore, the input–output relation in the time domain can be represented as :

$$k\dot{x}+k(c+2a-2\alpha)x$$
$$+\int_0^t x(\tau)g^*(t-\tau)d\tau=y(t) \tag{16}$$

where $g^*(t)$ is a normalized impulse response function which results from elimination of the singularities from $g(t)$ in Eq. (15).

If the frequency response function $\hat{g}(\omega)$ is obtained experimentally, parameters a, b, c, k, α and β in Eqs. (13) and (14) can be identified by using least–mean–squares method. Thus, one can evaluate the pressure integrals as a frequency response function $\hat{g}(\omega)$, a transfer function $\hat{g}(s)$, and an impulse response function $g(t)$.

4. Transient Maneuver Test

One generally operates a P. M. M. so as to make pure sway and pure yaw motions. However, in transient state, it is difficult to control the P. M. M. such that drift angle coincides with yaw angle of the model. To overcome this difficulty, we have designed a P. M. M. which gives pure sway motion and combined motion of sway and yaw in a transient state. This is shown in Fig. 1. This P. M. M. consists of a lateral sliding bed for swaying and a vertical shaft for yawing which are controlled by D. C. servo–motors respectively. The vertical shaft is attached to a model at the center of gravity so that it is free from sinkage and trim. Maximum swaying amplitude is 300 mm and the maximum yawing amplitude is 20 degrees. The lateral force and moment acting on the model are measured by a dynamometer mounted in the model and the motions of swaying and yawing by potentiometers mounted in the lateral sliding bed. All data is recorded simultaneously in a microcomputer. Finally the complex frequency response function can be computed by taking the Fourier transform of the motion and the force or the moment.

In the transient motion of pure sway mode

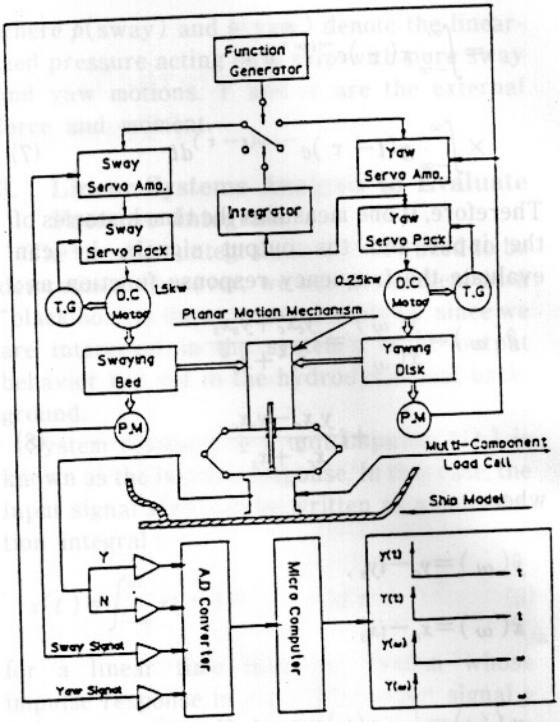

Fig. 1 Planar motion mechanism for transient maneuvering tests.

the model is controlled to move laterally in impulsive motion while the center line of the model is forced to point the direction of the carriage's motion. This eliminates, as a result, yawing motion ; the model is limited to swaying transient motion. The measured lateral force and yaw moment are only related to sway velocity and acceleration. For this mode, from Eq. (2), one obtains :

$$m\dot{v}+\iint_s p(\text{sway})n_y dS=Y(\text{sway})$$
$$\iint_s p(\text{sway})(xn_y-yn_x)dS=N(\text{sway}) \tag{17}$$

Taking the Fourier transform of Eq. (17) :

$$i\omega m+\frac{\iint_s \hat{p}(\text{sway})n_y dS}{\hat{v}(\omega)}=\frac{\hat{Y}(\text{sway})}{\hat{v}(\omega)}$$

$$\frac{\iint_s \hat{p}(\text{sway})(xn_y - yn_x)dS}{\hat{v}(\omega)} = \frac{\hat{N}(\text{sway})}{\hat{v}(\omega)} \tag{18}$$

where $\hat{v}(\omega)$, $\hat{Y}(\text{sway})$ and $\hat{N}(\text{sway})$ are the Fourier transforms of measured sway velocity $v(t)$, lateral force $Y(\text{sway})$ and moment $N(\text{sway})$. An example of the experiments are shown in Fig. 2.

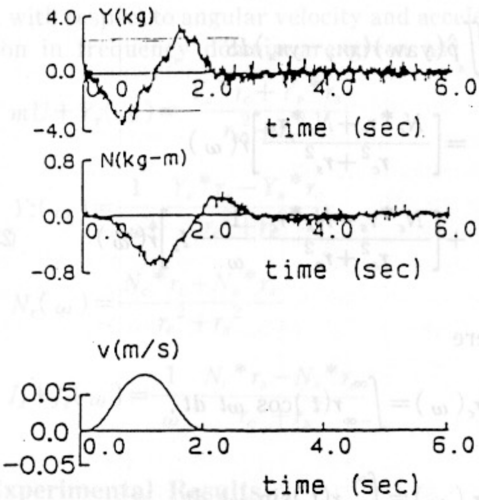

Fig. 2 Time history of transient sway test.

Thus, the pressure integrals in frequency domain can be evaluated as:

$$\iint_s \hat{p}(\text{sway})n_y dS$$

$$= \left[\frac{Y_c(\text{sway})v_c + Y_s(\text{sway})v_s}{v_c^2 + v_s^2}\right]\hat{v}(\omega)$$

$$+ \left[\frac{Y_c(\text{sway})v_s - Y_s(\text{sway})v_c}{v_c^2 + v_s^2}\frac{1}{\omega}\right.$$

$$\left. -m\right]\hat{\dot{v}}(\omega)$$

$$\iint_s \hat{p}(\text{sway})(xn_y - yn_x)dS$$

$$= \frac{N_c(\text{sway})v_c + N_s(\text{sway})v_s}{v_c^2 + v_s^2}\hat{v}(\omega)$$

$$+ \frac{N_c(\text{sway})v_s - N_s(\text{sway})v_c}{v_c^2 + v_s^2}\frac{1}{\omega}\hat{\dot{v}}(\omega) \tag{19}$$

where

$$v_c = \int_{-\infty}^{\infty} v(t)\cos\omega t\, dt,$$

$$v_s = \int_{-\infty}^{\infty} v(t)\sin\omega t\, dt,$$

$$Y_c(\text{sway}) = \int_{-\infty}^{\infty} Y(\text{sway})\cos\omega t\, dt,$$

$$Y_s(\text{sway}) = \int_{-\infty}^{\infty} Y(\text{sway})\sin\omega t\, dt,$$

$$N_c(\text{sway}) = \int_{-\infty}^{\infty} N(\text{sway})\cos\omega t\, dt,$$

$$N_s(\text{sway}) = \int_{-\infty}^{\infty} N(\text{sway})\sin\omega t\, dt,$$

$$\hat{\dot{v}} = i\omega\hat{v}(\omega) \tag{20}$$

From Eq. (19), the hydrodynamic derivatives $Y_v(\omega)$, $N_v(\omega)$, $N_{\dot{v}}(\omega)$ and added mass $m_y(\omega)$ with respect to sway velocity and acceleration in the frequency domain are given as:

$$Y_v(\omega) = \frac{Y_c(\text{sway})v_c + Y_s(\text{sway})v_s}{v_c^2 + v_s^2}$$

$$m + m_y(\omega) = \frac{1}{\omega}\,\frac{Y_c(\text{sway})v_s - Y_s(\text{sway})v_c}{v_c^2 + v_s^2}$$

$$N_v(\omega) = \frac{N_c(\text{sway})v_c + N_s(\text{sway})v_s}{v_c^2 + v_s^2}$$

$$N_{\dot{v}}(\omega) = \frac{1}{\omega}\,\frac{N_c(\text{sway})v_s - Y_s(\text{sway})v_c}{v_c^2 + v_s^2} \tag{21}$$

In the cases of combined motion of sway and yaw, the motion are more complex. As well as the model is controlled to move laterally, the heading is controlled to move simultaneously in the direction of the drift angle. Thus, the model experiences yaw velocity and acceleration in addition to sway velocity and acceleration. The measured forces and moments are related to sway and yaw velocities and to accelerations. Taking the Fourier transform of Eq. (2):

$$\left[i\omega m+\frac{\iint_s \hat{p}(\mathrm{sway})n_y dS}{\hat{v}(\omega)}\right]\hat{v}(\omega)$$

$$+\left[mU+\frac{\iint_s \hat{p}(\mathrm{yaw})n_y dS}{\hat{r}(\omega)}\right]\hat{r}(\omega)=\hat{Y}(\omega)$$

$$\frac{\iint_s \hat{p}(\mathrm{sway})(xn_y-yn_x)dS}{\hat{v}(\omega)}\hat{v}(\omega)$$

$$+\left[i\omega I_z+\frac{\iint_s \hat{p}(\mathrm{yaw})(xn_y-yn_x)dS}{\hat{r}(\omega)}\right]\hat{r}(\omega)$$

$$=\hat{N}(\omega) \qquad (22)$$

where $\hat{v}(\omega)$, $\hat{r}(\omega)$, $\hat{Y}(\omega)$ and $\hat{N}(\omega)$ are the Fourier transforms of measured sway velocity $v(t)$, yaw velocity $r(t)$, lateral force $Y(t)$ and yaw moment $N(t)$. An example of the experiments in this mode is shown in Fig. 3.

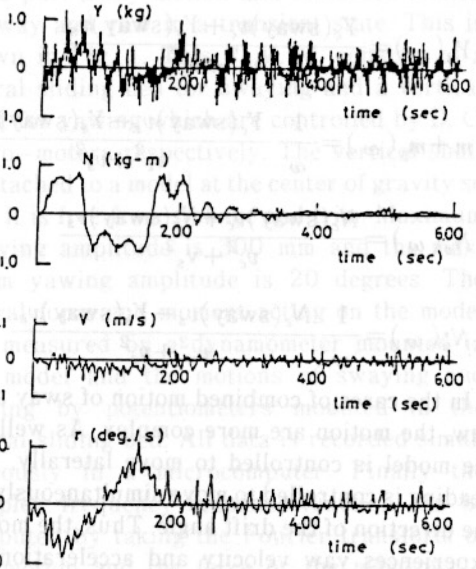

Fig. 3 Time history of transient combined motion test.

As before, the pressure integrals of pure yaw can be evaluated as:

$$\iint_s \hat{p}(\mathrm{yaw})n_y dS$$

$$=\left[\frac{Y_c{}^*r_c+Y_s{}^*r_s}{r_c{}^2+r_s{}^2}-mU\right]\hat{r}(\omega)$$

$$+\left[\frac{Y_c{}^*r_s-Y_s{}^*r_c}{r_c{}^2+r_s{}^2}\frac{1}{\omega}\right]\hat{\dot{r}}(\omega)$$

$$\iint_s \hat{p}(\mathrm{yaw})(xn_y-yn_x)dS$$

$$=\left[\frac{N_c{}^*r_c+N_s{}^*r_s}{r_c{}^2+r_s{}^2}\right]\hat{r}(\omega)$$

$$+\left[\frac{N_c{}^*r_s-N_s{}^*r_c}{r_c{}^2+r_s{}^2}\frac{1}{\omega}-I_z\right]\hat{\dot{r}}(\omega) \qquad (23)$$

where

$$r_c(\omega)=\int_{-\infty}^{\infty}r(t)\cos\omega t\,dt,$$

$$r_s(\omega)=\int_{-\infty}^{\infty}r(t)\sin\omega t\,dt,$$

$$Y_c(\omega)=\int_{-\infty}^{\infty}Y(t)\cos\omega t\,dt,$$

$$Y_s(\omega)=\int_{-\infty}^{\infty}Y(t)\sin\omega t\,dt,$$

$$N_c(\omega)=\int_{-\infty}^{\infty}N(t)\cos\omega t\,dt,$$

$$N_s(\omega)=\int_{-\infty}^{\infty}N(t)\sin\omega t\,dt,$$

$$Y_c{}^*(\omega)=Y_c(\omega)-Y_v(\omega)v_c(\omega)$$

$$-[m+m_y(\omega)]\,\omega v_s(\omega)$$

$$Y_s{}^*(\omega)=Y_s(\omega)-Y_v(\omega)v_s(\omega)$$

$$+[m+m_y(\omega)]\,\omega v_c(\omega),$$

$$N_c^*(\omega)=N_c(\omega)-N_v(\omega)v_c(\omega)$$

$$-\omega N_v^{\cdot}(\omega)v_s(\omega)$$

$$N_s^*(\omega)=N_s(\omega)-N_v(\omega)v_s(\omega)$$

$$+\omega N_v^{\cdot}(\omega)v_c(\omega) \tag{24}$$

From Eq. (23), the hydrodynamic derivatives Y_r, $Y_r^{\cdot}$, N_r and the added moment of inertia J_z with respect to angular velocity and acceleration in frequency domain are given as:

$$mU+Y_r(\omega)=\frac{Y_c^*r_c+Y_s^*r_s}{r_c^2+r_s^2}$$

$$Y_r^{\cdot}(\omega)=\frac{1}{\omega}\frac{Y_c^*r_s-Y_s^*r_c}{r_c^2+r_s^2}$$

$$N_r(\omega)=\frac{N_c^*r_c+N_s^*r_s}{r_c^2+r_s^2}$$

$$I_z+J_z(\omega)=\frac{1}{\omega}\frac{N_c^*r_s-N_s^*r_c}{r_c^2+r_s^2} \tag{25}$$

Experimental Results

Model tests were conducted, based on the preceeding analysis. A model of a container ship was used, and her dimensions and profile are shown in Table 1 and in Fig. 4. The model ship is towed at a velocity of 1.11 m/s or Froude number of 0.224.

Table 1 Principal particulars of the ship and the model.

Items		Ship	Model
Length	(m)	115.0	2.5
Breadth	(m)	19.0	0.413
Draft	(m)	6.4	0.139
Displaced volume	(m)	9859.0	0.101
Wetted surface area	(m)	2845.0	1.345
Block coefficient		0.705	0.705
Midship section coef.		0.970	0.970
Breadth/Draft ratio		2.97	2.97
Length/Breadth ratio		6.05	6.05
Model Scale			1/46

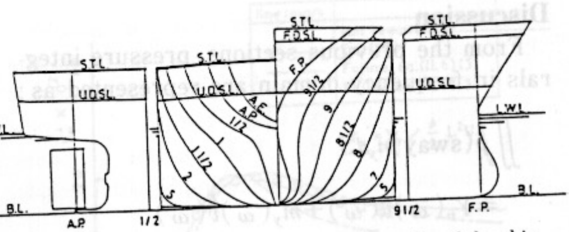

Fig. 4 Body plan, and bow and stern profile of the ship model.

From the time histories as shown in Figs. 2 and 3, the non-dimensional hydrodynamic derivatives Y_v', $m'+m_y'$, N_v' and $N_v^{\cdot\prime}$ for sway, and $m'+Y_r'$, $Y_r^{\cdot\prime}$, N_r', $I_z'+J_z'$ for yaw are determined through a few trials as shown in Figs. 5 and 6, respectively. For all cases the results are in good agreement with those obtained by the usual P. M. M. indicated by circles in the figures.

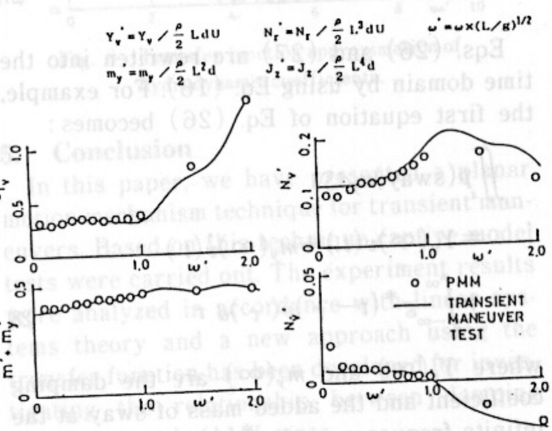

Fig. 5 Results of transient sway tests.

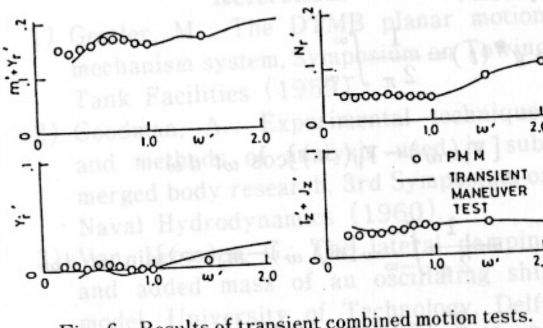

Fig. 6 Results of transient combined motion tests.

Discussion

From the previous sections, pressure integrals in frequency domain are represented as:

$$\iint_s \hat{p}(\text{sway}) n_y dS$$

$$= Y_v(\omega)\hat{v}(\omega) + m_y(\omega)\hat{\dot{v}}(\omega)$$

$$\iint_s \hat{p}(\text{sway})(x n_y - y n_x) dS$$

$$= N_v(\omega)\hat{v}(\omega) + N_{\dot{v}}(\omega)\hat{\dot{v}} \tag{26}$$

and

$$\iint_s \hat{p}(\text{yaw}) n_y dS$$

$$= Y_r(\omega)\hat{r}(\omega) + Y_{\dot{r}}(\omega)\hat{\dot{r}}(\omega)$$

$$\iint_s \hat{p}(\text{yaw})(x n_y - y n_x) dS$$

$$= N_r(\omega)\hat{r}(\omega) + J_z(\omega)\hat{\dot{r}} \tag{27}$$

Eqs. (26) and (27) are rewriten into the time domain by using Eq. (16). For example, the first equation of Eq. (26) becomes:

$$\iint_s p(\text{sway}) n_y dS$$

$$= Y_v(\infty) v(t) + m_y(\infty)\dot{v}(t)$$

$$+ \int_{-\infty}^{\infty} g^*(t-\tau) v(\tau) d\tau \tag{28}$$

where $Y_v(\infty)$ and $m_y(\infty)$ are the damping coefficient and the added mass of sway at the infinite frequency, and $g^*(t)$ is its normalizing impulse response function. For a causal system:

$$g^*(t) = \frac{1}{2\pi}\int_{-\infty}^{\infty}$$

$$[Y_v(\omega) - Y_v(\infty)]\cos \omega t \, d\omega$$

$$-\frac{1}{2\pi}\int_{-\infty}^{\infty} \omega[m_y(\omega) - m_y(\infty)]\sin \omega t \, d\omega$$

$$= \frac{2}{\pi}\int_0^{\infty} [Y_v(\omega) - Y_v(\infty)]\cos \omega t \, d\omega$$

$$-\frac{2}{\pi}\int_0^{\infty} \omega[m_y(\omega) - m_y(\infty)]\sin \omega t \, d\omega \tag{29}$$

Fujino[9] has shown that the Kramers–Kronig relation between damping coefficient and added mass for a maneuvering ship can be given as:

$$m_y(\omega) - m_y(\infty) = -\frac{1}{\pi \omega}\int_{-\infty}^{\infty} \frac{Y_v(k)}{\omega - k} dk$$

$$Y_v(\omega) - Y_v(0) = \frac{\omega}{\pi}\int_{-\infty}^{\infty} \frac{m_y(k)}{\omega - k} dk \tag{30}$$

However, it is rather difficult to calculate Eq. (30), because exact values of damping coefficient and added mass cannot be obtained at the infinite frequency. Thus, a transfer function approximation is introduced to analyze experiment results.

Assuming second order polynomials for both the denominator and the numerator of the transfer function just as Eq. (12) the damping coefficient $Y_v(\omega)$ and added mass $m_y(\omega)$ can be described as:

$$Y_v(\omega)$$

$$= k\left[\frac{c\{(b^2-\omega^2)(\beta^2-\omega^2) + 4\omega^2 a\alpha\}}{(\beta^2-\omega^2)^2 + 4\omega^2\alpha^2}\right.$$

$$\left. - \frac{2\omega^2\{a(\beta^2-\omega^2) - \alpha(b^2-\omega^2)\}}{(\beta^2-\omega^2)^2 + 4\omega^2\alpha^2}\right]$$

$$m + m_y(\omega)$$

$$= k\left[\frac{(b^2-\omega^2)(\beta^2-\omega^2) + 4\omega^2 a\alpha}{(\beta^2-\omega^2)^2 + 4\omega^2\alpha^2}\right.$$

$$\left. - \frac{2c\{a(\beta^2-\omega^2) - \alpha(b^2-\omega^2)\}}{(\beta^2-\omega^2)^2 + 4\omega^2\alpha^2}\right] \tag{31}$$

and

$$\lim_{\omega \to 0} Y_v(\omega) = kc(b/\beta)^2$$

$$\lim_{\omega \to \infty} m_y(\omega) = k \tag{32}$$

$Y_v(0)$ is the derivative experimentally determined from an oblique tow test, but other parameters k, a, b, c, α and β are unknown.

So, these parameters are identified from the experiment results using least–mean–squares method. Thus, one can directly evaluate the compatibility of damping coefficient $Y_v(\omega)$ and added mass $m_y(\omega)$.

Fig. 7 shows this relation. The circles represent the experiment results and the solid lines are evaluated using Eq. (31). The results are in excellent agueement. Eq. (31) seems to be more useful than the Kramers–Kronig relations, because one can determine and investigate damping and added mass coefficients from the limited range of frequency. Calculation at infinite frequency are not required.

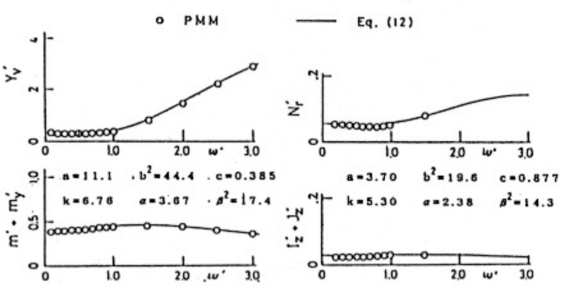

Fig. 7 Kramers–Kroning relations.

We have used the same approach to re–evaluated experiments by van Leeuwen. This is shown in Fig. 8. The circles are results obtained by van Leeuwen[3], the one–dot chain lines are Fujino's approximated function[9], the two–dot chain lines are Fujino's calculation of Eq. (30) using the approximation function each other, and the solid lines are estimated by Eq. (31). The approximate transfer function in Eq. (12) accurately expresses the damping coefficient and the added mass of sway. The main difference between Fujino's approximation function and Eq. (12) is whether the same set of parameters are used to represent the properties of damping and added mass coefficients or not. In other words, both damping and added mass coefficients are represented by the same set of parameters in Eq. (12) as shown in Eq. (31). Thus it is no longer necessary to verify results by the Kramers–Kronig relations.

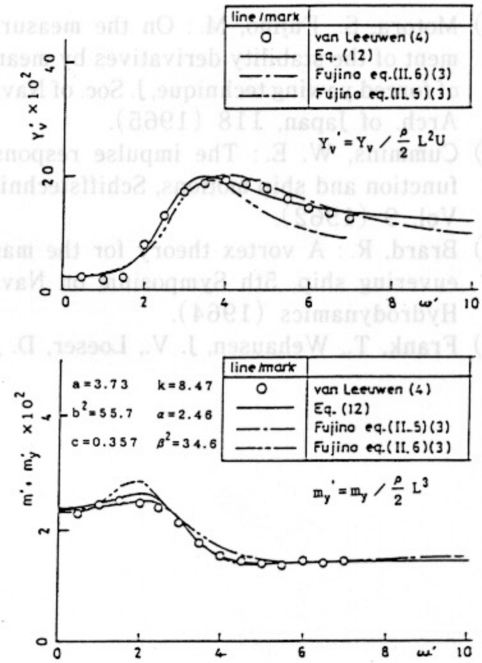

Fig. 8 Transfer function approximation of hydrodynamic coefficients.

5. Conclusion

In this paper, we have presented a planar motion mechanism technique for transient maneuvers. Based on this technique captive model tests were carried out. The experiment results were analyzed in accordance with linear systems theory and a new approach using the transfer function has been developed for investigating the relationship between damping coefficient and added mass.

References

1) Gertler, M.: The DTMB planar motion mechanism system, Symposium on Towing Tank Facilities (1959).

2) Goodman, A.: Experimental techniques and methods of analysis used in submerged body research, 3rd Symposium on Naval Hydrodynamics (1960).

3) Van. Leeuwen, G.: The lateral damping and added mass of an oscillating ship model, University of Technology, Delft, Report of Shipbuilding Laboratory, No. 23 (1964).

4) Motora, S., Fujino, M.: On the measurement of the stability derivatives by means of forced yawing technique, J. Soc. of Naval Arch. of Japan, 118 (1965).
5) Cummins, W. E.: The impulse response function and ship motions, Schiffstechnik, Vol. 9 (1962).
6) Brard, R.: A vortex theory for the maneuvering ship, 5th Symposium on Naval Hydrodynamics (1964).
7) Frank, T., Wehausen, J. V., Loeser, D. J., Scragg, C. A., Sibul, O. J. and Webster, W. C.: Transient–maneuver testing and the equations of maneuvering, 11th Symposium on Naval Hydrodynamics (1976).
8) Martin, L. L.: Discussion to the Paper of Bishop, R. E. D. *et al.*, 10th Symposium on Naval Hydrodynamics (1974) p. 122.
9) Fujino, M.: The effect of frequency dependence of the stability derivatives on maneuvering motion, I. S. P., Vol. 22, No. 256 (1975).